

Role of cross-helicity in magnetohydrodynamic turbulence

Jean Carlos Perez¹ and Stanislav Boldyrev¹

¹*Department of Physics, University of Wisconsin-Madison,
1150 University Ave, Madison, WI 53706, USA*

(Dated: October 24, 2018)

Strong incompressible three-dimensional magnetohydrodynamic turbulence is investigated by means of high resolution direct numerical simulations. The simulations show that the configuration space is characterized by regions of positive and negative cross-helicity, corresponding to highly aligned or anti-aligned velocity and magnetic field fluctuations, even when the average cross-helicity is zero. To elucidate the role of cross-helicity, the spectra and structure of turbulence are obtained in ‘imbalanced’ regions where cross-helicity is non-zero. When averaged over regions of positive and negative cross-helicity, the result is consistent with the simulations of balanced turbulence. An analytical explanation for the obtained results is proposed.

PACS numbers: 52.35.Ra

Introduction.—Magnetohydrodynamic (MHD) turbulence has been a starting point for modeling large-scale turbulent motion of plasmas in a wide variety of settings, ranging from laboratory experiments to astrophysical systems, [e.g., 1]. When written in terms of the Elsässer variables the incompressible MHD equations read

$$\left(\frac{\partial}{\partial t} \mp \mathbf{v}_A \cdot \nabla\right) \mathbf{z}^\pm + (\mathbf{z}^\mp \cdot \nabla) \mathbf{z}^\pm = -\nabla P, \quad (1)$$

where the Elsässer variables are defined as $\mathbf{z}^\pm = \mathbf{v} \pm \mathbf{b}$, \mathbf{v} is the fluctuating plasma velocity, \mathbf{b} is the fluctuating magnetic field normalized by $\sqrt{4\pi\rho_0}$, $\mathbf{v}_A = \mathbf{B}_0/\sqrt{4\pi\rho_0}$ is the contribution of the uniform magnetic field \mathbf{B}_0 , $P = (p/\rho_0 + b^2/2)$ includes the plasma pressure p and the magnetic pressure, and ρ_0 is the background plasma density that we assume constant. It follows from these equations that for $\mathbf{z}^\mp(\mathbf{x}, t) = 0$, an arbitrary function $\mathbf{z}^\pm(\mathbf{x}, t) = F^\pm(\mathbf{x} \pm \mathbf{v}_A t)$ is an exact nonlinear solution that represents a non-dispersive wave propagating along the direction $\mp \mathbf{v}_A$. Nonlinear interactions are thus the result of collisions between counter-propagating Alfvén waves.

The first phenomenological picture of MHD turbulence was proposed independently by Iroshnikov [2, 3] and Kraichnan [4] (IK), who predicted an inertial range scaling of the isotropic energy spectrum $E(k) \sim k^{-3/2}$. In this picture, the spectral energy transfer at a given scale $\lambda \sim 1/k$ results from the cumulative effect of multiple weak interactions between counter-propagating Alfvén wave packets moving along the magnetic field of the large-scale energy containing eddies. One shortcoming of this phenomenology is that it is based on the assumption of an isotropic spectral transfer, in clear contradiction with recent results that reveal the anisotropic character of MHD turbulence [e.g., 1, 5, 6]. Indeed, Galtier et.al. [7] applied the formalism of weak turbulence to equations (1), demonstrating that the spectral transfer is much more efficient in the field-perpendicular plane, and derived a steeper energy spectrum $E(k_\perp) \propto k_\perp^{-2}$,

where k_\perp is the field perpendicular wave-number. This scaling was originally predicted in [8, 9, 10] based on more phenomenological grounds.

As the cascade proceeds to smaller scales, the eddies become progressively more elongated in the field-parallel direction, and the nonlinear interaction becomes stronger. Eventually, the so called ‘critical balance’ condition of Goldreich and Sridhar (GS) [11] is established. This condition states that the turbulence is considered strong when there is a formal balance between the crossing time of two interacting Alfvén wave packets and the characteristic nonlinear interaction time, i.e., $k_\parallel B_0 \sim k_\perp b_\lambda$, where k_\parallel is the typical field-parallel wave-number of the fluctuations spectrum, and b_λ is the rms magnitude of the fluctuations at the scale $\lambda \sim 1/k_\perp$. The resulting scaling in the GS picture is $E(k_\perp) \sim k_\perp^{-5/3}$.

The explosive growth of massively parallel computers in recent years has made direct numerical simulations of MHD equations a valuable tool for studying fundamental properties of MHD turbulence. For instance, simulations indicate that the scaling of the energy spectrum of strong MHD turbulence is anisotropic, as in GS picture, but with the scaling of the IK phenomenology [12, 13, 14, 15, 16]. In order to resolve this controversy, it has been proposed [17, 18] that magnetic and velocity fluctuations tend to align their polarizations in turbulent eddies, leading to scale-dependent depletion of nonlinear interaction of Alfvén modes. This leads to the anisotropic energy spectrum $E(k_\perp) \sim k_\perp^{-3/2}$, in agreement with numerical simulations.

The phenomenon of scale-dependent dynamic alignment is closely related to the conservation of cross-helicity, an ideal invariant cascading toward small scales in a turbulent state. Cross-helicity has only recently become an object of systematic study, as it became clear that it plays a fundamental role in driven MHD turbulence [14, 15, 17, 18, 19, 20, 21, 22, 23].

Denote $E^\pm = \langle |\mathbf{z}^\pm|^2 \rangle / 4$ the energy associated with the \pm waves, then the total energy and cross-helicity of the

system are $E = E^+ + E^-$ and $H_c = E^+ - E^-$, respectively. Both energy and cross-helicity are invariants of the ideal MHD equations. Cross-helicity provides a measure of the imbalance between non-linearly interacting waves. When it does not vanish the turbulence is called *imbalanced*, otherwise it is *balanced*.

A significant interest to imbalanced MHD turbulence has also been motivated by astrophysical solar wind data, which indicate that solar wind turbulence is dominated by Alfvén waves propagating outward from the sun [e.g., 24]. A number of analytic derivations of the spectra of imbalanced MHD turbulence have been recently proposed [19, 20, 21, 22], which however lead to contradictory results. Most of numerical simulations of MHD turbulence have so far concentrated on balanced cases, and practically no systematic study of strong imbalanced MHD turbulence in high-resolution direct numerical simulations has been available.

In an attempt to address the issue and to resolve the contradictions, we performed high resolution numerical simulations to investigate the inertial range of strong MHD turbulence with and without cross-helicity. Based on our results, we propose that in the imbalanced case the Elsässer energy spectra have different amplitudes, nevertheless, their scaling is the same, $E^+(k_\perp) \propto E^-(k_\perp) \propto k_\perp^{-3/2}$. This scaling coincides with the scaling in the balanced case, which is consistent with the view that balanced MHD turbulence is as a superposition of locally imbalanced regions. We demonstrate that this picture is essentially consistent with the phenomenon of scale-dependent dynamic alignment, and provide an analytic explanation for the obtained spectra.

Model equations.— The universal properties of weak and strong turbulence in MHD are accurately described by neglecting the parallel component of the fluctuating fields, associated with the pseudo-Alfvén mode [16, 25]. By setting $\mathbf{z}_\parallel^\pm = 0$ in equation (1) we obtain the closed system of equations

$$\left(\frac{\partial}{\partial t} \mp \mathbf{v}_A \cdot \nabla_\parallel\right) \mathbf{z}^\pm + (\mathbf{z}^\mp \cdot \nabla_\perp) \mathbf{z}^\pm = -\nabla_\perp P + \mathbf{f}^\pm + \nu \nabla^2 \mathbf{z}^\pm, \quad (2)$$

in which force and dissipation terms have been added to address the case of steadily driven turbulence, and we assume that viscosity is equal to resistivity. This set of equations is known as the Reduced MHD model (RMHD) [26, 27]. It is worth mentioning that the RMHD model was derived as an approximation of the full MHD equations in the limit $k_\parallel \ll k_\perp$, and therefore it is applicable to strong turbulence. It has been recently realized that when used in a broader $k_\parallel - k_\perp$ domain the system (2) describes the universal regime of *weak* Alfvénic turbulence [16]. This opens the possibility of effective analytic and numerical study of both weak and strong MHD turbulence in the same framework. In the present paper, we

Run	Resolution	Re	α	L_\parallel/L_\perp	n_\parallel	ρ_c
A	$1024^2 \times 256$	4000	0.	6	1	0
B	$512^2 \times 256$	1500	0.3	5	2	0.6
C1	512^3	1500	0.25	10	2	0.6
C2	$1024^2 \times 256$	4000	0.25	10	2	0.6

TABLE I: Summary of simulations. A, B, C correspond to strong turbulence with different amount of net cross-helicity.

use this system to study strong anisotropic MHD turbulence.

Numerical method.—We employ a fully dealiased Fourier pseudo-spectral method to solve equations (2) with a strong guide field ($v_A/v_{rms} \sim 5$) in a rectangular periodic box, with field-perpendicular cross section $L_\perp^2 = (2\pi)^2$ and field-parallel box size L_\parallel . The choice of a rectangular box, as discussed in [16], allows for the excitation of elongated modes at large scales, necessary to avoid a long transition region from the forcing to the inertial interval, which can lead to inaccurate measurements of the spectral index.

In order to achieve a steady state, the random forcing \mathbf{f}^\pm is applied in Fourier space at wave-numbers $1 \leq k_\perp \leq 2, (2\pi/L_\parallel) \leq k_\parallel \leq (2\pi/L_\parallel)n_\parallel$, where n_\parallel controls the width of the force spectrum in k_\parallel . The Fourier coefficients inside that range are Gaussian random numbers with amplitude chosen so that the resulting rms velocity fluctuations are of order unity. The individual random values are refreshed independently for each mode on average every $\tau = 0.1 L_\perp/v_{rms}$. As shown in [16], the width of the field-parallel spectrum controls the critical balance at the forcing scale, and determines whether the turbulence is weak or strong. We define the Reynolds number as $Re = (L_\perp/2\pi)v_{rms}/\nu$.

In the present simulations, we also introduce correlation between \mathbf{v} and \mathbf{b} , to investigate the role of cross-helicity. Such correlation is introduced at the forcing scales by controlling the correlation between the velocity and magnetic field forces, \mathbf{f}_v and \mathbf{f}_b . This is achieved by taking \mathbf{f}^\pm as uncorrelated Gaussian random forces, so that $\mathbf{f}_v = \frac{1}{2}(\mathbf{f}^+ + \mathbf{f}^-)$, $\mathbf{f}_b = \frac{1}{2}(\mathbf{f}^+ - \mathbf{f}^-)$, from which it immediately follows that cross-helicity is controlled by the difference in the variances: $\langle \mathbf{f}_v \cdot \mathbf{f}_b \rangle = \frac{1}{4}(\sigma_+^2 - \sigma_-^2)$, where $\sigma_\pm^2 \equiv \langle |\mathbf{f}^\pm|^2 \rangle$. It is convenient to define the parameter α and the normalized cross helicity:

$$\alpha \equiv (\sigma_+^2 - \sigma_-^2)/(\sigma_+^2 + \sigma_-^2) = 2\langle \mathbf{f}_v \cdot \mathbf{f}_b \rangle, \quad (3)$$

$$\rho_c \equiv H_c/E = (E^+ - E^-)/(E^+ + E^-) \quad (4)$$

Results.—Table I shows the summary of three representative simulations. Runs A, B, C were carried out with narrow k_\parallel -band forcing that produces critically balanced and strongly interacting large-scale modes. The energy spectra are shown in Fig. 1, compensated by

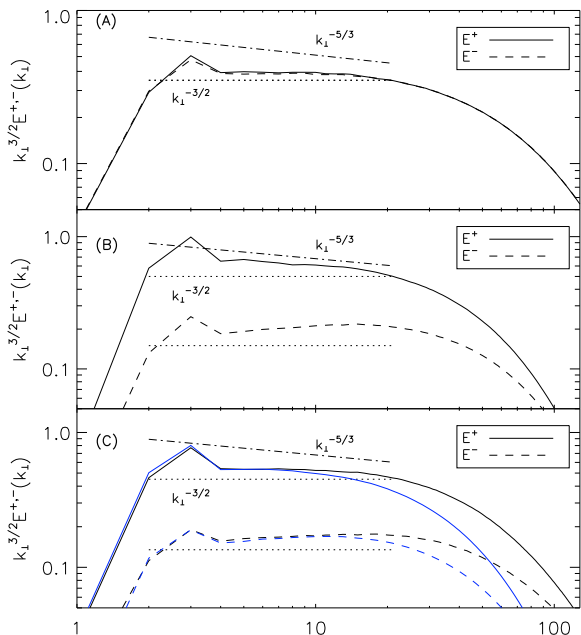


FIG. 1: Spectra of balanced and imbalanced strong turbulence corresponding to runs A, B, C1 (blue) and C2 (black) (see the text). In plots (B) and (C), the spectrum of z^- is arbitrarily offset in the vertical direction.

$k_{\perp}^{3/2}$. In run A with $\alpha = 0$, we observe a balanced turbulence with the scaling close to $E^+ \sim E^- \sim k_{\perp}^{-3/2}$. When cross-helicity is introduced in Run B, we observe a slight steepening of $E^+ \sim k_{\perp}^{-1.6}$ and a slight flattening of $E^- \sim k_{\perp}^{-1.35}$. This behavior is justified as follows: since the total energy $E = E^+ + E^-$ is kept constant, when the cross-helicity increases, the amplitude of \mathbf{z}^+ increases at the expense of \mathbf{z}^- . Therefore, the nonlinear interaction of \mathbf{z}^+ with \mathbf{z}^- becomes weaker, resulting in a steepening of the spectrum. This steepening is however an artifact of a not optimal numerical setting. To simulate this interaction correctly, we need to elongate the box in field-parallel direction so as to fit the eddies with longer parallel wavelengths at the forcing scales. As a result, the E^{\pm} spectra get closer to $k_{\perp}^{-3/2}$; this is evident in Runs C1 and C2. Note that the limit of very large cross-helicity would require extremely long simulation box in order to observe the universal scaling behavior $k_{\perp}^{-3/2}$.

Discussion.—In this section we propose an explanation for the observed spectra. Our explanation essentially relies on the phenomenon of scale-dependent dynamic alignment. To understand how the alignment affects the energy spectrum, consider the eddy shown in Fig. 2. In this eddy fluctuations are aligned within the small angle θ_{λ} , while their directions and magnitudes change in an almost perpendicular direction. In the case of strong balanced turbulence, the nonlinear interaction in such an eddy is then reduced by a factor θ_{λ} for both z^+ and z^-

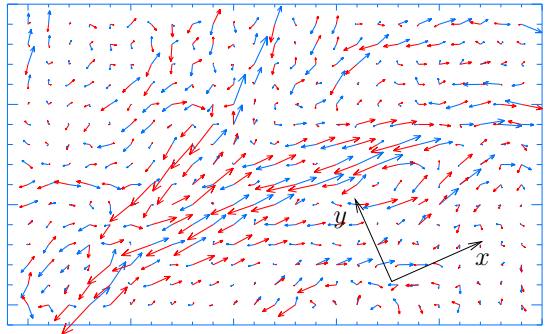


FIG. 2: A correlated region of (counter-)aligned magnetic and velocity fluctuations (red and blue vectors) at scale $\lambda = L_{\perp}/12$, in a plane perpendicular to the strong guide field, in run A. The fluctuations are aligned predominantly in the x direction while their directions and amplitudes change predominantly in the y direction.

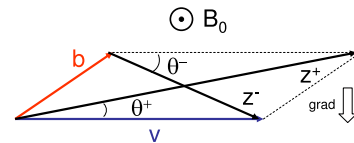


FIG. 3: Sketch of dynamic alignment of magnetic and velocity fluctuations in a turbulent eddy.

fields, and the corresponding nonlinear interaction time is estimated as $\tau_{\lambda} \sim 1/(\mathbf{z}_{\lambda}^{\pm} \cdot \mathbf{k}_{\perp}) \sim 1/(z_{\lambda}^{\pm} k_{\perp} \theta_{\lambda})$. The scaling of the fluctuating fields is then found from the requirement of constant energy fluxes: $(z_{\lambda}^{\pm})^2/\tau_{\lambda} = \text{const}$. One can argue [14, 15, 18] that the alignment angle decreases with scale as $\theta_{\lambda} \propto \lambda^{1/4}$, in which case the field-perpendicular energy spectrum is $E(k_{\perp}) \propto k_{\perp}^{-3/2}$.

In the case of strong imbalanced turbulence, the alignment is still preserved. However, since the fields amplitudes are essentially different the alignment angles are different as well; we denote them θ_{λ}^+ and θ_{λ}^- , see Fig. 3. The assumption of the dynamic alignment then leads to the important geometric constraint: $\theta_{\lambda}^+ z_{\lambda}^+ \sim \theta_{\lambda}^- z_{\lambda}^-$, as is clear from Fig. 3. The depletion of nonlinear interaction is therefore different for z^+ and z^- fields, however, their nonlinear interaction times, $\tau_{\lambda}^{\mp} \sim 1/(z_{\lambda}^{\pm} k_{\perp} \theta_{\lambda}^{\pm})$, are the same. The requirement of constant energy fluxes $(z_{\lambda}^{\pm})^2/\tau_{\lambda}^{\pm} \sim \epsilon^{\pm} = \text{const}$ then ensures that $z_{\lambda}^+/z_{\lambda}^- \sim \sqrt{\epsilon^+/\epsilon^-}$, so both fields should have the same scaling, although different amplitudes. The geometric constraint then leads to $\theta_{\lambda}^+/\theta_{\lambda}^- \sim \sqrt{\epsilon^-/\epsilon^+}$, so the alignment angles should have the same scaling as well.

To conclude this section we compare our results with recent analytic predictions of Lithwick et al. [20], Beresnyak and Lazarian [22], and Chandran [21]. The main difference of our model with previous studies is that we include the phenomenon of dynamic alignment. In [20]

the energy cascade times were assumed to be essentially different and the derived spectra had the form $E^+(k_\perp) \propto E^- \propto k_\perp^{-5/3}$, while our numerical results are more consistent with $k_\perp^{-3/2}$. In [21, 22], it was assumed that the z^+ field undergoes a weak cascade, while z^- a strong cascade, leading to different spectra of z^+ and z^- , which seems to be supported by numerical simulations in [22]. We however note that the steepening of the z^+ and the flattening of the z^- spectra might be due to the high level of cross-helicity in these simulations (around $\rho_c \sim 0.97$), which requires an extremely elongated simulation box in the field-parallel direction, cf. our Fig. 1(B). In addition, the simulations in [22] are performed on lower resolution with hyperviscosity, which might alter the spectra due to a bottleneck effect.

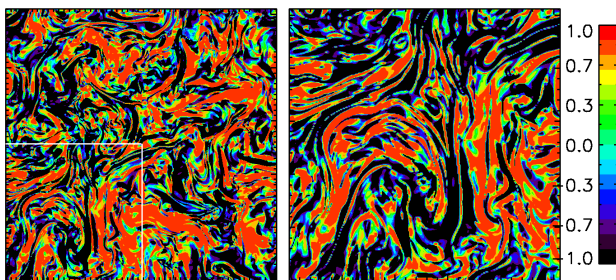


FIG. 4: Cosine of the alignment angle between \mathbf{v}_λ and \mathbf{b}_λ fluctuations in the guide-field perpendicular plane at scales $\lambda = L_\perp/6$ (left), and $\lambda = L_\perp/12$ (right) in Run A. The right frame corresponds to the region delimited by the white square on the left side.

Conclusion.—We have presented the results of numerical simulations of strong MHD turbulence in both balanced and imbalanced regimes. In the imbalanced turbulence, say with positive cross-helicity, the total energy spectrum $E = E^+ + E^-$ is dominated by E^+ . Simulations in this case show a universal inertial-range regime: although the E^+ and E^- spectra have different amplitudes, their scaling is the same $E^+(k_\perp) \propto E^-(k_\perp) \propto k_\perp^{-3/2}$.

In the balanced turbulence, both spectra have the same amplitudes and scaling $E^+(k_\perp) \sim E^-(k_\perp) \sim k_\perp^{-3/2}$. This is consistent with the view that overall balanced turbulence can be imbalanced locally, creating patches (eddies) of positive and negative cross-helicity. In each of these regions the picture of imbalanced turbulence presented above applies. When averaged over all the regions, the spectra of balanced turbulence are reproduced.

The presented picture of MHD turbulence is consistent with the phenomenon of scale-dependent dynamic alignment [17, 18], which provides a natural explanation for the observed spectra. In this phenomenology, the configuration space splits into eddies with highly aligned and anti-aligned magnetic and velocity fluctuations, where nonlinear interactions are reduced. Fig. 4 shows the cosine of the alignment angle between veloc-

ity and magnetic fluctuations for the balanced simulations (run A), at scales $\lambda = L_\perp/6$ and $\lambda = L_\perp/12$. The alignment possesses a hierarchical structure: inside small eddies there exist smaller and more anisotropic eddies (of both polarities), and so on. This hierarchical structure, first observed by Mason & Cattaneo [unpublished, 2006], presents an interesting example of magnetic self-organization in a driven turbulent system.

This work was supported by the U.S. DOE under Grant No. DE-FG02-07ER54932, by the NSF Center for Magnetic Self-Organization in Laboratory and Astrophysical Plasmas at the UW-Madison, and in part by the NSF under Grant No. NSF PHY05-51164. High Performance Computing resources were provided by the Texas Advanced Computing Center (TACC) at the University of Texas at Austin under the NSF-Teragrid Project TG-PHY080013N.

-
- [1] D. Biskamp, *Magnetohydrodynamic Turbulence* (Cambridge University Press, Cambridge, 2003).
 - [2] P. S. Iroshnikov, *AZh* **40**, 742 (1963).
 - [3] P. S. Iroshnikov, *Sov. Astron* **7**, 566 (1964).
 - [4] R. H. Kraichnan, *Phys. Fluids* **8**, 1385 (1965).
 - [5] J. V. Shebalin, W. H. Matthaeus, and D. J. Montgomery, *J. Plasma Physics* **29**, 525 (1983).
 - [6] D. Montgomery and L. Turner, *Phys. Fluids* **24**, 825 (1981).
 - [7] S. Galtier, S. V. Nazarenko, A. C. Newell, and A. Pouquet, *J. Plasma Physics* **63**, 447 (2000).
 - [8] C. S. Ng and A. Bhattacharjee, *ApJ* **465**, 845 (1996).
 - [9] A. Bhattacharjee and C. S. Ng, *ApJ* **548**, 318 (2001).
 - [10] C. S. Ng, A. Bhattacharjee, K. Germaschewski, and S. Galtier, *Phys. Plasmas* **10**, 1954 (2003).
 - [11] P. Goldreich and S. Sridhar, *ApJ* **438**, 763 (1995).
 - [12] J. Maron and P. Goldreich, *ApJ* **554**, 1175 (2001).
 - [13] W.-C. Müller and R. Grappin, *Phys. Rev. Lett.* **95**, 114502 (2005).
 - [14] J. Mason, F. Cattaneo, and S. Boldyrev, *Phys. Rev. Lett.* **97**, 255002 (2006).
 - [15] J. Mason, F. Cattaneo, and S. Boldyrev, arXiv:0706.2003 (2007).
 - [16] J. C. Perez and S. Boldyrev, *ApJ* **672**, L61 (2008).
 - [17] S. Boldyrev, *ApJ* **626**, L37 (2005).
 - [18] S. Boldyrev, *Phys. Rev. Lett.* **96**, 115002 (2006).
 - [19] Y. Lithwick and P. Goldreich, *ApJ* **582**, 1220 (2003).
 - [20] Y. Lithwick, P. Goldreich, and S. Sridhar, *ApJ* **655**, 269 (2007).
 - [21] B. Chandran, *Astrophys. J.* **685**, 646 (2008).
 - [22] A. Beresnyak and A. Lazarian, *ApJ* **682**, 1070 (2008).
 - [23] W. H. Matthaeus, A. Pouquet, P. D. Mininni, P. Dmitruk, and B. Breech, *Phys. Rev. Lett.* **100**, 085003 (2008).
 - [24] D. A. Goldstein, D. A. Roberts, and W. H. Matthaeus, *Annu. Rev. Astron. Astrophys.* **33**, 283 (1995).
 - [25] S. Galtier and B. D. G. Chandran, *Phys. Plasmas* **13**, 114505 (2006).
 - [26] B. B. Kadomtsev and O. P. Pogutse, *Sov. Phys.- JETP* **38**, 283 (1974).

[27] H. R. Strauss, *Phys. Fluids* **19**, 134 (1976).